($k_2$) associated with rigid body motion, are equal in number to the independent element displacements.

For conformability in subsequent matrix operations, the matrix $[\bar{U}]$ is expanded with columns of zeros to accommodate the coefficients $\{k_2\}$ as well as $\{k_1\}$ and is redesignated as $[U]$. Thus, Eq. (1) can be restated as

$$\{\sigma\} = [U]\{k\} \tag{1a}$$

Through integration of the stresses over the surface of the element, stress resultants $\{p\}$ at the chosen points can be defined in terms of the coefficients $\{k\}$:

$$\{p\} = [V]\{k\} \tag{4}$$

The matrix $[V]$ also contains sufficient zero columns to accommodate the coefficients $\{k_2\}$ and therefore the postmultiplier $\{k\}$. Combining Eqs. (3) and (4), one has

$$\{p\} = [V][B]^{-1}\{\Delta\} \tag{5}$$

Hence, the desired stiffness matrix $[S]$ is established as

$$[S] = [V][B]^{-1} \tag{6}$$

To develop the second alternative, begin with the virtual work definition of an individual stiffness coefficient[3]

$$S_{ij} = \int_V [\sigma_i]\{\varepsilon_j\}dV \tag{7}$$

where $[\sigma^i]$ is the stress vector due to a *unit* displacement at $i$, $\{\varepsilon_j\}$ is the strain vector due to a *unit* displacement at $j$, and $dV$ is a differential volume of the element whose total volume is $V$. Stress-strain relations can be written in the form

$$\{\varepsilon\} = [N]\{\sigma\} \tag{8}$$

so that (7) becomes

$$S_{ij} = \int_V [\sigma_i][N]\{\sigma_j\}dV \tag{7a}$$

Combining (1a) with (3) and designating $\{\Delta_j\}$ as a column vector with 1.0 in the $j$ place and zeros elsewhere gives

$$\{\sigma_j\} = [U][B]^{-1}\{\Delta_j\} \tag{9}$$

and, through transposition, with the superscript $T$ signifying the transpose of the indicated matrices,

$$\{\sigma_i\} = [\Delta_i]([B]^{-1})^T[U]^T \tag{9a}$$

Hence, one can write (7a) as (the $[B]$ matrix is unaffected by the integration)

$$S_{ij} = [\Delta_i]([B]^{-1})^T\left[\int_V [U]^T[N][U]dV\right][B]^{-1}\{\Delta_j\} \tag{7b}$$

By direct reasoning, it follows that

$$[S] = ([B]^{-1})^T[G][B]^{-1} \tag{10}$$

where

$$[G] = \left[\int_V [U]^T[N][U]dV\right] \tag{11}$$

Summarizing the formations established here and in Ref. 1, one has the following:

1) From virtual work (virtual forces), indirectly, via the derivation of the flexibility matrix and inversion thereof,

$$[\bar{S}] = [\bar{V}][\bar{G}]^{-1}[\bar{V}]^T \tag{12}$$

$$\left([\bar{G}] = \left[\int_V [\bar{U}]^T[N][\bar{U}]dV\right]\right) \tag{13}$$

[As indicated earlier, in connection with Eqs. (1) and (1a), matrices with bars over their designating symbols exclude only the terms associated with rigid body motion of the element.]

2) From "direct formulation,"

$$[S] = [V][B]^{-1} \tag{6}$$

3) From virtual work (virtual displacements) via direct derivation

$$[S] = ([B]^{-1})^T[G][B]^{-1} \tag{10}$$

In the virtual forces approach, the result is dependent upon the transformation matrix $[\bar{V}]$ of the edge stresses into stress resultants; displacement transformations (idealizations) do not appear. Consequently, displacements corresponding to the chosen stress field may violate compatibility. Conversely, the virtual displacement approach depends upon the displacement transformation matrix $[B]$, excludes the stress-to-corner force transformation matrix $[V]$, and can be used in developments based on assumed displacements whose counterpart stresses violate the conditions of equilibrium. The direct formulation, Eq. (6), involves both the force and displacement transformations and nothing else.

All three approaches will yield identical element relationships for simple conditions, e.g., prismatic members governed by elementary flexure, triangular plates under constant plane stress, etc. This does not necessarily hold for complex geometric conditions and assumed behavior representations such as arbitrary quadrilaterals under direct stress or bending. Furthermore, under the latter conditions, a straightforward derivation of a symmetric $[S]$ matrix through use of Eq. (6) may prove difficult to achieve. $[S]$ matrices derived via Eqs. (10) and (12) must be symmetric, since the indicated matrix products are congruent transformations with $[G]$ and $[\bar{G}]$ symmetric matrices. Developments starting with strain energy theorems (Castigliano's first theorem) also lead to Eqs. (10) and (12). Each row of $[G]$, for example, will be an equation for the derivative of the strain energy (expressed in terms of the coefficients $k$) with respect to one of the coefficients $k$.

### References


[1] Best, G. C., "A formula for certain types of stiffness matrices of structural elements," AIAA J. 1, 212–213 (1963).

[2] Gallagher, R. H., "A correlation study of methods of matrix structural analysis," AGARDograph 69 (July 1962).

[3] Argyris, J. H. and Kelsey, S., *Energy Theorems and Structural Analysis* (Butterworths Scientific Publications Ltd., London, 1960).


---

# Supersonic Interference Lift


F. Mysliwetz*

*United Aircraft Corporation, East Hartford, Conn.*



**It is shown that the interference lift of a body-wing combination proposed and analyzed previously can be higher than originally anticipated. Whitham's theory is adapted to predict the load distribution induced on the wing by the body.**


RESEARCH on favorable supersonic interference of lifting wingbody systems has attracted considerable interest in recent years.[1, 2] Since it is possible to improve aerodynamic efficiency at supersonic speeds by using the lift


Received March 5, 1963. The experimental data were obtained while the author was with the Boeing Airplane Co. The author also wishes to thank F. A. Woodward from Boeing and J. H. Clarke from Brown University for valuable discussions on that subject.



* Research Engineer, Research Laboratories. Member AIAA.

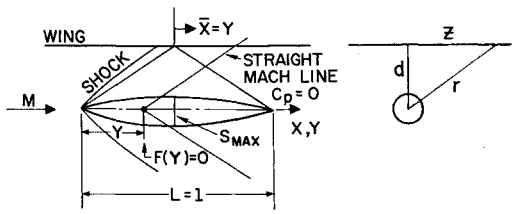


**Fig. 1 Body-wing interference configuration**

created by some of the aircraft components (fuselage, nacelles, external stores, etc.) due to favorable interference with the wing, a body-wing combination incorporating this feature was proposed and analyzed in Ref. 1. It consisted of a body of revolution (Sears-Haack body) suspended beneath a wing in such a position that the pressure field of the body induced additional lift on the wing (Fig. 1). Such a body-wing interference system is further investigated below.

In this analysis the angles of attack of wing and body are both assumed to be zero, and the wing-body distance $d$ is such that the reflections from the wing do not influence the body (Fig. 1). Experiments with a Sears-Haack body of revolution underneath a flat plate at supersonic Mach numbers show good correlation with the theoretical interference lift (Fig. 2) given in Ref. 1 as

$$L/qS_{\max} = 2S(y)/\alpha S_{\max} \qquad (1)$$

$$x = y + \alpha d \qquad \alpha = (M^2 - 1)^{1/2}$$

where $M$ is the freestream Mach number, $S(y)$ is the body cross section at $y$, $S_{\max}$ is the maximum body cross section, and $q$ is the freestream dynamic pressure. This equation was derived from integral relations, based on linearized theory, which do not require a knowledge of the pressure field. Equation (1) indicates that the interference lift reaches its maximum value if the body from the tip to its maximum cross section is allowed to influence the wing. However, a still larger interference lift can be obtained with the same configuration. An examination of the pressure distribution on the wing reveals an extensive area of negative lift which diminishes the influence of the positive lift (Fig. 3). Elimination of this negative lift area by a wing cutout along a line where the pressure coefficient is zero results in a steady rise of the interference lift with wing chord (Fig. 2) beyond the maximum value given by Eq. (1).

In order to determine the total positive interference lift, a detailed knowledge of the pressure distribution in the wing plane is required. Since linearized theory for slender bodies becomes inadequate for a detailed description of the flow away from the body axis, a more accurate theory is necessary. The projectile theory of Whitham[3] gives a good approximation to the flow everywhere and therefore was used in the foremention interference problem. The pressure coefficient in the flow field of the projectile on the modified char-

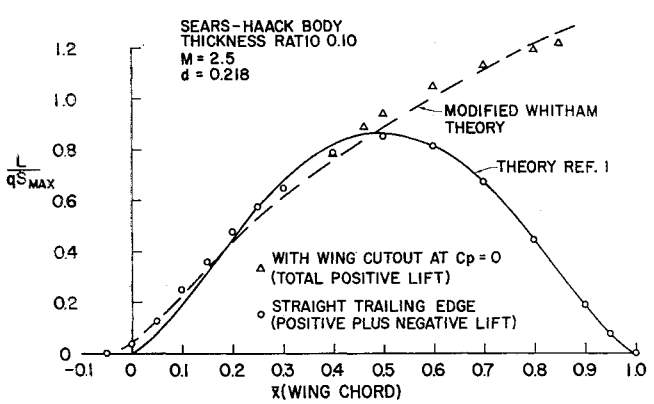


**Fig. 2 Interference lift on the wing**

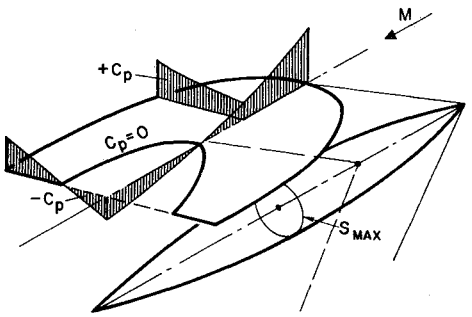


**Fig. 3 Load distribution on the wing**

acteristics with

$$K = 2.4M^4/(2\alpha^3)^{1/2} \qquad x = y + \alpha r - KF(y)r^{1/2} \qquad (2)$$

is given by Whitham's theory

$$C_p = 2F(y)/(2\alpha r)^{1/2} \qquad (3)$$

For pointed bodies with continuous first and second derivatives of the cross-sectional area $S'(x)$ and $S''(x)$, the function $F(y)$ has the following form:

$$F(y) = \frac{1}{2\pi}\int_0^y \frac{S''(x)dx}{(y-x)^{1/2}} \qquad (4)$$

The variable $y$ in the forementioned formulas is defined as the characteristic variable.[3] In order to obtain the pressure coefficient in the wing plane, the pressure distribution has to be doubled in order to account for the reflections (the problem can be considered as a mirror image problem). Thus the interference pressure coefficient becomes

$$C_{pI} = 4F(y)/(2\alpha r)^{1/2} \qquad (5)$$

The experimental results of Fig. 4 show good agreement with the load distribution calculated by use of Eq. (5). The boundary between the positive and negative load on the wing can be described by the intersection of the wing with a Mach cone (freestream Mach angle) originating at the body axis at the point where the function $F(y)$ is zero. With $F(y) = 0$ the pressure coefficient becomes zero; and from Eq. (2) it may be seen that the locus of $C_{pI} = 0$ in the wing plane is the intersection of a freestream Mach cone with the wing. The bow shock given by Whitham's theory stands ahead of the actual shock wave, particularly at Mach numbers in excess of two. Therefore the theoretically predicted wing area

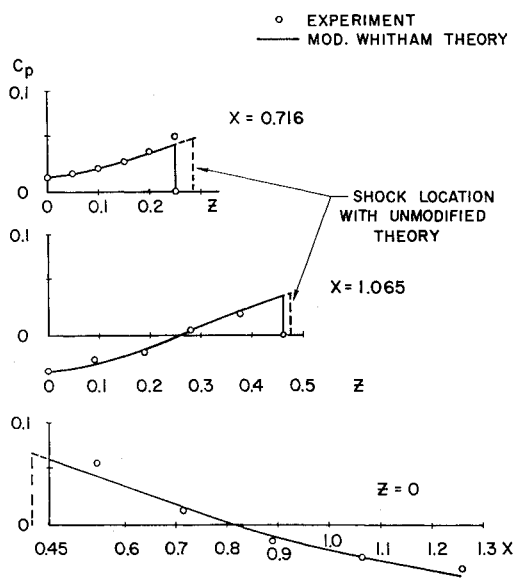


**Fig. 4 Spanwise and chordwise pressure distribution on the wing at $M = 2.5$**

influenced by the body becomes larger than the actual one. In order to correct for this a shock shape must be introduced which closely approximates the actual shock. In the example of Fig. 2, at a Mach number of 2.5, a conical shock shape was used. The agreement between experimental and theoretical values of interference lift is good (Fig. 2).

The feature of the negative pressure coefficient ahead of the maximum cross section of the body, and the resulting negative interference lift region previously described is exhibited by most of the parabolic and power-law bodies of revolution (minimum drag bodies) used in supersonic flow. Therefore, it should be considered in the analysis and optimization of the forementioned interference configuration.

There is no effect of the wing upon the body for the spacing just considered. For closer spacing there is a negative lift acting on the body; however, the lift on the wing increases, and the total lift is still positive.

### References

[1] Ferri, A., Clarke, J. H., and Ting, L., "Favorable interference in lifting systems in supersonic flow," J. Aeronaut. Sci. **24**, 791–804 (1957).

[2] Chen, C. F. and Clarke, J. H., "Body under lifting wing," J. Aerospace Sci. **28**, 547–562 (1961).

[3] Whitham, G. B., "The flow pattern of a supersonic projectile," Communs. Pure and Appl. Math. **5**, 301–348 (1952).

## Magnetic Induction Parameter for Lorentz Accelerators

HERBERT BECKMANN*
*Rice University, Houston, Texas*

THE thrust per unit cross section area $p_f$ developed by Lorentz accelerators is in the first approximation equal to the cross product of the magnetic induction $B$ and the linear electric current density $j$ measured in the transverse plane of the flow:

$$p_f = j \times B = \dot{m}(v_2 - v_1) \tag{1}$$

It is also equal to the change in momentum of the working fluid with a mass flow density of $\dot{m}$ and with entrance and exit velocities of $v_1$ and $v_2$, respectively. Equation (1) is valid for the range in which secondary effects are negligible, i.e., as long as the magnetic induction $B$ is small. The optimum amount of $B$ which produces maximum thrust output with a given electric current density depends, therefore, on secondary effects. Inclusion of phenomena such as ion slip and Hall currents in the derivation of Eq. (1) leads to a complicated analysis.[1]

A different approach to this problem can be based on the hypothesis that secondary effects become significant when high efficiencies in the energy conversion process are attempted. The optimum amount for $B$ can be determined directly from the change of available electric energy into kinetic energy of the working fluid. The electric power input per unit cross section area of the accelerator $q$ has to be equal to or greater than the increase in kinetic energy of the working fluid plus the power required to increase its degree of ionization by the fraction $\Delta\alpha$:

$$q \geq \epsilon\dot{m}\Delta\alpha + 0.5\dot{m}(v_2^2 - v_1^2) \tag{2}$$

with $\epsilon$ being the ionization (and dissociation) energy of the working fluid. Equations (1) and (2) are combined to eliminate $v_2$:

$$(j \times B)/\dot{m} \leq \{2\epsilon[(q/\dot{m}\epsilon) - \Delta\alpha] + v_1^2\}^{1/2} - v_1 \tag{3}$$

Equation (3) can be used to determine the proper amount of the magnetic induction $B$ for the experiment. Demetriades[2] and Ziemer determined the optimum amount of $B$ experimentally for the specific conditions of their test stand and obtained $B = 1840$ gauss. Equation (3) yields for the same test conditions $B = 1780$ gauss, if a (certainly too large) $\Delta\alpha = 1$ is assumed arbitrarily. The experimentally determined amount of $B = 1840$ gauss, when introduced into Eq. (3), results for this specific test condition in a $\Delta\alpha = 0.75$ instead of the here-assumed $\Delta\alpha = 1$.

In the event that cross-field accelerators with high thrust output are under consideration, Eq. (3) can be simplified by neglecting $v_1$ and $\Delta\alpha$ against the other terms, and a magnetic performance parameter $\sigma$ can be established:

$$\sigma = B(j/E\dot{m})^{1/2} = Bh(I/VM)^{1/2} \leq 2^{1/2} \tag{4}$$

with $E$ being the voltage potential. In the second term, the distance $h$, the voltage drop $V$, and the total current $I$ are measured between the electrodes of the accelerator, and $M$ designates the total mass flow rate through the unit. This parameter $\sigma$ may turn out to be useful not only in comparing performance characteristics of different $j \times B$ accelerators but also in the adjustment and calibration of local nonuniformities in the properties of the same unit.

### References

[1] Demetriades, S. T., Hamilton, G. L., Ziemer, R. W., and Lenn, P. D., "Three-fluid nonequilibrium plasma accelerators (Part 1)," *AIAA Progress in Astronautics and Aeronautics: Electric Propulsion Development* (Academic Press, New York, 1963), Vol. 9, pp. 461–511.

[2] Demetriades, S. T. and Ziemer, R. W., "Direct thrust and efficiency measurements of a continuous plasma accelerator," ARS J. **31**, 1278–1280 (1961).

Received March 6, 1963.

* Professor of Mechanical Engineering. Member AIAA.

## Earth Albedo Input to Flat Plates

F. G. CUNNINGHAM*
*NASA Goddard Space Flight Center, Greenbelt, Md.*

**In this short note, the results of an analysis considering the earth reflected solar radiation incident upon a spinning flat plate are presented briefly. A general description of the problem is given, as well as a definition of all of the geometrical parameters, even though the final result itself is not given explicitly. However, the final integral expression is given, as well as the expressions for determining the integration limits. In actual practice, it proves to be rather easy to perform the integration with the aid of a computer. The parameters introduced succeed in defining the orientation of the surface with respect to the earth. No attempt is made here to give these parameters in terms of orbital parameters. Even so, unfortunately, it would not relieve the reader from the troublesome task of determining the remainder of the parameters from analysis of such data as time of launch, point of launch, injection angle, etc., for any particular problem that he may wish to consider.**

### Nomenclature

$S$ = mean solar constant
$\mathbf{s}$ = solar vector

Received March 8, 1963.

* Physicist, Thermal Systems Branch, Spacecraft Technology Division.